JPET Fast Forward. Published on November 7, 2016 as DOI: 10.1124/jpet.116.237214
This article has not been copyedited and formatted. The final version may differ from this version.

Low Potential of Basimglurant to be involved in Drug-Drug Interactions: Influence of non-Michaelis-Menten CYP Kinetics on Fraction Metabolized.

Stephen Fowler, Elena Guerini, NaHong Qiu, Yumi Cleary, Neil Parrott, Gerard Greig and Navita L. Mallalieu*

Roche Pharma Research and Early Development, Roche Innovation Center Basel, 4070 Basel, Switzerland

*****Corresponding author, Roche Innovation Center New York City, USA

a) Running title: Basimglurant drug-drug interactions

b) Corresponding Author

Navita L. Mallalieu

Roche Pharma Research and Early Development,

Roche Innovation Center New York City,

430 East 29th Street

New York, New York 10016

USA Phone: +1 646-461-5165

Fax: +1 646-461-5175

E-mail: navita_l.mallalieu@roche.com

c) Numbers

Number of Text Pages: ~19

Number of Tables: 2

Number of Figures: 4

Number or References: 49

Number of words in the Abstract: 238

Number of words in the Introduction: 682

Number of words in the Discussion: 1511

JPET Fast Forward. Published on November 7, 2016 as DOI: 10.1124/jpet.116.237214
This article has not been copyedited and formatted. The final version may differ from this version.

d) Abbreviations

AUC_{inf} Area under the plasma concentration vs. time curve extrapolated to infinity

AUC_{last} Area under the plasma concentration vs. time curve up to the last measured data-point

C_{max} Maximum plasma concentration

CYP Cytochrome P450 isozyme

DDI Drug-Drug Interaction

HIM Human intestinal microsomes

HLM Human liver microsomes

NADPH β-Nicotinamide adenine dinucleotide phosphate (reduced form)

PK Pharmacokinetics

e) Recommended section:

Metabolism, Transport, and Pharmacogenomics

JPET Fast Forward. Published on November 7, 2016 as DOI: 10.1124/jpet.116.237214
This article has not been copyedited and formatted. The final version may differ from this version.

Abstract

Basimglurant, a novel mGlu5 negative allosteric modulator under development for the treatment of major depressive disorder, is cleared via cytochrome P450 (CYP) mediated oxidative metabolism. Initial enzyme phenotyping studies indicated that CYP3A4/5 dominated basimglurant metabolism and highlighted a risk for drug-drug interactions when comedicated with strong CYP3A4/5 inhibitors or inactivators. However, a clinical drug-drug interaction (DDI) study using the potent and selective CYP3A4/5 inhibitor ketoconazole resulted in an AUCi/AUC ratio of only 1.24. A further study using the CYP3A4 inducer carbamazepine resulted in an AUCi/AUC ratio of 0.69. More detailed in vitro enzyme phenotyping and kinetics studies showed that, at the low concentrations attained clinically, basimglurant metabolic clearance is catalyzed mainly by CYP1A2. The relative contributions of the enzymes were estimated as 70:30 CYP1A2:CYP3A4/5. Using this information, a clinical study using the CYP1A2 inhibitor fluvoxamine was performed, resulting in an AUCi/AUC ratio of 1.60 confirming the role of CYP1A2 and indicating a balanced DDI risk profile. Basimglurant metabolism kinetics show enzyme dependency: CYP1A2 mediated metabolism follows Michaelis-Menten kinetics, whilst CYP3A4 and CYP3A5 follow sigmoidal kinetics (with similar K_M and S_{50} values). The interplay of the different enzyme kinetics leads to changing fractional enzyme contributions to metabolism with substrate concentration, even though none of the metabolic enzymes are saturated. This example demonstrates the relevance of non Michaelis-Menten CYP enzyme kinetics and highlights the need for thorough understanding of metabolism enzymology to make accurate predictions for human metabolism in vivo.

JPET Fast Forward. Published on November 7, 2016 as DOI: 10.1124/jpet.116.237214
This article has not been copyedited and formatted. The final version may differ from this version.

Introduction

Regulatory guidelines recommend that enzymes contributing more than 25% to the clearance of a new drug molecule should be identified and drug-drug interaction (DDI) risk associated with their inhibition assessed (EMA, 2012; FDA, 2012). A combination of in vitro drug metabolism experiments followed up by clinical pharmacology studies is typically used to establish the metabolism enzymology of a new drug. This information can then be used to assess the genetic polymorphism and DDI risks. Following this paradigm, it is essential that in vitro enzyme phenotyping studies (Zhang et al., 2007; Zientek and Youdim, 2015) provide data which are effective predictors for the clinical situation. In the event of inconsistency between in vitro and clinical study findings, it is important that a feedback loop exists to allow the clinical findings to be addressed in a mechanistic way and for additional studies to be performed to test and confirm new hypotheses. Thus, a consistent and comprehensive understanding of the clearance of a new drug molecule can be reached and allow effective guidance to be made to physicians regarding any medications which must be contraindicated and any dose adjustments which may need to be made in order to safely administer the medicines.

Non Michaelis-Menten kinetics has been observed for many drug-metabolizing enzymes, including UDP-glucuronosyltransferases, sulfotransferases and CYPs (Uchaipichat et al., 2004; Huang et al., 2009; Wu, 2011; Gufford et al., 2016). Deviation from Michaelis-Menten kinetics may be observed in the form of homotropic cooperativity (sigmoidal kinetic forms) and substrate inhibition effects. Such behavior is frequently encountered in CYP3A4 catalyzed reactions (Shou et al., 2001; Hutzler and Tracy, 2002; Atkins, 2005). This is thought to be due to the capability of the large CYP3A4 active site to accommodate more than one substrate molecule simultaneously (Shou et al., 1994; Fowler et al., 2002; Williams et al., 2004; Yano et al., 2004) and that the presence of

JPET Fast Forward. Published on November 7, 2016 as DOI: 10.1124/jpet.116.237214
This article has not been copyedited and formatted. The final version may differ from this version.

additional substrate (or effector) molecules in the active site may either enhance or suppress the rate of substrate turnover (Atkins, 2005). Despite many examples of non Michaelis-Menten kinetics demonstrated in vitro, there is scant evidence for measurable influence on in vivo pharmacokinetics or drug-drug interactions.

Depression as a major cause of disability worldwide (Ferrari et al., 2013). Results from a large scale trial to evaluate depression treatment (STAR*-D), showed that only one-third of patients achieved remission with initial treatment, and remission rates declined even further with each successive treatment attempt (Rush et al., 2006). Moreover, various switching strategies employed as second-line treatments did not yield improved results (Rush et al., 2006). Failure to obtain remission, therefore, is a common clinical problem. The cause of major depression is multi factorial, and includes elements of social and psychological development, genetics, and the proposed dysfunction in several neurotransmitter pathways. In recent years, evidence has accumulated for the importance of deregulated cortical glutamatergic pathways in major depression (Manji et al., 2003; Zarate and Tohen, 2004; Zarate et al., 2006b; Connolly and Thase, 2012; Duman et al., 2012; Quiroz JA, 2012; Licznerski and Duman, 2013), and evidence of the antidepressant effects of anti-glutamatergic drugs such as ketamine in pilot clinical trials (Berman et al., 2000; Zarate et al., 2006a). Given the psychotogenic effects and associated risk of addiction ketamine posesses (Krystal et al., 2013), mGlu5 negative allosteric modulators offer an alternative target for investigation (Chaki et al., 2013).

Basimglurant, an orally active selective mGlu5 negative allosteric modulator was developed for the treatment of Major Depressive Disorder (MDD) in conjunction with standard antidepressants. In functional magnetic resonance imaging experiments in rats, basimglurant triggered antidepressant associated changes in brain activity pattern (Lindemann et al., 2015). Basimglurant also elicited dose-dependent anxiolytic-like

effects in the stress induced hyperthermia model in mice and showed activity in antidepressant-like rat models, including the forced swim test, as well as the chronic mild stress and anhedonia model (Jaeschke et al., 2015; Lindemann et al., 2015). Basimglurant has been administered either as immediate release (IR) hard gelatin capsules or as modified release (MR) formulations in a number of Phase I and II trials. Results from a large (N = 333) randomized phase II clinical trial evaluating the efficacy and safety of basimglurant as adjunctive therapy for major depression demonstrated multiple positive endpoints (Quiroz et al., 2016).

The aim of the presently reported studies was to assess the risk for basimglurant to be subject to drug-drug interactions both in vitro and in vivo and to understand the mechanistic basis for the results obtained. This report highlights the importance of having a detailed understanding of drug metabolism kinetics and of using clinically relevant drug substrate concentrations to allow the best chance for in vitro enzymology studies results to be extrapolated to the in vivo situation.

JPET Fast Forward. Published on November 7, 2016 as DOI: 10.1124/jpet.116.237214
This article has not been copyedited and formatted. The final version may differ from this version.

Materials and Methods

Materials

α-Naphthoflavone, fluvoxamine, ketoconazole, NADPH, quercetin, quinidine, *S*-mephenytoin, sulfaphenazole, tacrine and testosterone were purchased from Sigma-Aldrich (St Louis, MO, USA); Human hepatocytes (10-donor mixed gender pool) were purchased from BioReclamation / IVT (Brussels, Belgium); Human liver microsomes (150-donor mixed gender pool),recombinantly expressed CYP2E1 and UGT enzymes were purchased from Corning-Gentest (Woburn, MA, USA); human lung and kidney microsomes were purchased from Celsis-IVT (Brussels, Belgium); CYPs 1A1, 1A2, 2A6, 2B6, 2C8, 2C9, 2C19, 2D6, 3A4, 3A5 and 4A11 were generated at F. Hoffmann-La Roche Ltd (Basel, Switzerland) using *E*. coli with co-expression of cytochrome P450 reductase. (-)-N-3-Benzyl-phenobarbital was purchased from CYPex (Dundee, UK). Basimglurant, 14-C labelled basimglurant and basimglurant-M1 and -M2 metabolites were synthesised at F. Hoffmann-La Roche Ltd (Basel, Switzerland).

Enzymology Methods

Full details of the experimental parameters, including incubation volumes, incubation times and sample workup conditions, can be found in Supplementary Table 1. Details of the analytical methods used can be found in Supplementary Table 2. Below are the outline details of experimental designs for the various in vitro enzymology studies performed.

Recombinant CYP phenotyping: Incubations were made up in 100 mM potassium phosphate buffer, pH7.4 and contained a final concentration of 10 μM ^{14}C-basimglurant 200 pmol/mL P450, 1 mM NADPH and 0.5% v/v DMSO. Incubations containing a control

JPET Fast Forward. Published on November 7, 2016 as DOI: 10.1124/jpet.116.237214
This article has not been copyedited and formatted. The final version may differ from this version.

substance, typically at a final concentration of 20 µM (lauric acid, 25 µM), were made to ensure the activity of each enzyme and incubated in parallel. Turnover was calculated as percentage total chromatogram radioactivity in metabolite peaks using HPLC-radioflow analysis.

Recombinant UGT phenotyping: Reaction timecourse experiments with incubation times of 0.5, 3, 6, 10, 15, 20, 25 and 30 minutes were made up in 100 mM potassium phosphate buffer, pH7.4 and contained a final concentration of 1 or 10 µM basimglurant-M1 or basimglurant-M2, 1 mg/mL membrane protein expressing UGT enzyme, 5 mM UDPGA and 0.5% v/v DMSO. Incubations containing a control substance, at a final concentration of 10 µM, were made to ensure the activity of each enzyme and incubated in parallel. Glucuronide generation activities were assessed using LC-MS/MS and assessing the peak area ratios between glucuronide metabolite and internal standard. The average rates of reaction were normalised with the rate observed using pooled human liver microsomes set as 100%.

Kinetics: Incubations were performed in triplicate using 2-200 pmol/mL of the various CYPs or 0.25 mg/mL pooled human liver microsomes, 2.5 to 50 µM ^{14}C-basimglurant, 1 mM NADPH and 0.5% v/v DMSO in 100 mM potassium phosphate buffer, pH7.4. Incubations were prewarmed to 37 °C before reaction initiation by addition of NADPH. Reactions were quenched after 10-50 minutes (dependent upon the enzyme tested), centrifuged and sample supernatants further prepared and analyzed by radio-HPLC. The rates of M1 generation were calculated from the amount of radioactivity in the M1 metabolite peak as a percentage of total chromatogram radioactivity. Kinetic models (Michaelis-Menten, sigmoidal and substrate inhibition) were applied based upon inspection of the kinetic profiles and form of the data plotted on Eadie-Hofstee plots (insets in Figure 2).

JPET Fast Forward. Published on November 7, 2016 as DOI: 10.1124/jpet.116.237214
This article has not been copyedited and formatted. The final version may differ from this version.

Chemical Inhibition Experiments: A matrix of incubations was made up, in triplicate, containing 1 or 25 µM basimglurant, 10 µM tacrine, 20 µM S-mephenytoin or 30 µM testosterone as substrate and DMSO (vehicle control), 0.2 µM α-naphthoflavone, 2 µM benzylphenobarbital or 1 µM ketoconazole as inhibitors. Incubations contained 1 mg/mL HLM and 1 mM NADPH. Total incubation volumes were 300 µL. Incubations were prewarmed for 5 minutes to 37 °C before being started by addition of NADPH. Percentage control activity values were calculated for each of the incubations containing inhibitor using the HPLC-UV peak areas for metabolite M1 with the average of the DMSO control samples set as 100%.

Incubation with liver, lung and kidney microsomes: Basimglurant was incubated in triplicate at concentrations of 1 µM and 25 µM for 0, 15 and 60 minutes with 1 mg/mL microsomal protein and 1 mM NADPH at 37 °C in 100 mM phosphate buffer, pH7.4. Incubations were prewarmed for 5 minutes to 37 °C before being started by addition of NADPH. Amount of M1 generated was calculated for each of the incubations by calibrating the HPLC-UV peak areas for metabolite M1 against that of a chemically synthesized standard.

Basimglurant concentration dependence of chemical inhibition effect: A matrix of incubations was made up, in triplicate, containing (finally) 0.2, 0.4, 0.8, 1.6, 3.1, 6.3, 12.5 and 25 µM basimglurant combined with either 1 µM ketoconazole, 0.2 µM α-naphthoflavone or DMSO (as 100% activity control). Incubations contained 1 mg/mL HLM and 1 mM NADPH in 100 mM phosphate buffer pH7.4. Total incubation volumes were 500 µL. Incubations were prewarmed for 5 minutes to 37 °C before being started by addition of NADPH. Percentage control activity values were calculated for each of the incubations containing inhibitor using the HPLC-UV peak areas for metabolite M1 with the average of the DMSO control samples for the respective basimglurant concentration set as 100%. Under the experimental conditions used the inhibitors showed >85% on-

JPET Fast Forward. Published on November 7, 2016 as DOI: 10.1124/jpet.116.237214
This article has not been copyedited and formatted. The final version may differ from this version.

target inhibition effect and <15% off-target inhibition. Estimated values for the contributions of CYP1A2 and CYP3A4/5 were approximate and based upon the combined results of the inhibition studies performed and assuming essentially full and selective inhibition of the target CYPs by the chemical inhibitors.

Clinical Studies

Three dedicated clinical studies are described here. Each of the studies followed a similar design with an evaluation of effect of steady state exposure of an interacting drug on single dose pharmacokinetics of basimglurant. Each study was conducted as a single-center, open-label one-sequence cross-over design in 16 healthy male or female subjects 18 to 65 years of age (upper age limit of 50 years, n = 18 for the ketoconazole study). In each instance basimglurant was administered orally by itself initially to characterize single dose PK. In a second study period, multiple daily doses of the interacting drugs were administered over a period of 17 days (ketoconazole), 25 days (fluvoxamine) or 28 days (carbamazepine) and with a single dose basimglurant co-administered on the 7^{th} day (fluvoxamine), 5^{th} day (ketoconazole) and 14^{th} day (carbamazepine) to evaluate the impact of the interacting drug on the PK of basimglurant. Basimglurant was administered as single oral doses of 0.25 mg in the ketoconazole study, 0.2 mg in fluvoxamine study and 0.5 mg in the carbamazepine study. Different doses of basimglurant were employed in each study to ensure either that plasma levels would be measurable in case of induction and expected to be safe in case of inhibition. Doses of the interacting drugs employed were selected to ensure that adequate induction or inhibition would occur and were as follows: ketoconazole daily doses of 400 mg QD, carbamazepine daily doses of 400 mg BID (after a gradual escalation period prior to DDI investigation) and fluvoxamine daily evening doses of 100

JPET Fast Forward. Published on November 7, 2016 as DOI: 10.1124/jpet.116.237214
This article has not been copyedited and formatted. The final version may differ from this version.

mg QD (with a gradual tapering off after DDI investigation). Each of the interacting drugs were analysed using standard, validated specific LC-MS/MS analyses. Given the previously established tolerability findings regarding basimglurant, all three studies were conducted under fed conditions. There was a difference in the formulation employed among the studies. Since the ketoconazole study was the first study conducted an immediate release formulation was employed (Roche Clinical Studies Center, Strasbourg, France). Subsequently, in an attempt to improve tolerability a modified release formulation was developed and this formulation was employed in the fluvoxamine and carbamazepine DDI studies (Biotrial, Rennes, France). All studies were conducted in concordance with the ethical principles laid down in the declaration of Helsinki and with applicable local regulations and were approved by independent ethics committees. All subjects gave written informed consent before participating.

Pharmacokinetic blood samples were collected to characterize the PK of basimglurant when given by pre-dose, and at approximately 20 time points post dose over the next 12 days when given alone. A similar schedule was followed in the presence of the steady state concentrations of the interacting drug. Additional samples were taken in the second period to fully characterize the half-life of this slowly cleared drug over a total duration of 24-29 days post-dose. Samples were also taken to measure plasma levels of the interacting drug during the second period after multiple days of dosing in order to ensure that anticipated exposure was achieved.

The concentration of basimglurant in plasma was quantified using a validated LC-MS/MS method. The lower limit of quantification was 0.01 ng/mL; the calibration range 0.01 to 10 ng/mL. The precision and accuracy of the assay was 1.7% to 3.3% and 97.3% to 100.0% respectively. Pharmacokinetic parameters were estimated by non-compartmental analysis using WinNonlin Professional Edition 5.3 (Pharsight

JPET Fast Forward. Published on November 7, 2016 as DOI: 10.1124/jpet.116.237214
This article has not been copyedited and formatted. The final version may differ from this version.

Corporation, Mountain View, CA, USA); actual blood sampling times were used. Values below the limit of quantification before C_{max} were set to zero and after C_{max} to missing. The area under the concentration-time curve from time zero to the last measurable concentration post-dose (AUC_{last}) was calculated using the linear trapezoidal rule. The terminal half-life ($t_{1/2}$) and AUC_{inf} were calculated by estimating λ_z. The terminal elimination rate constant λ_z was assessed by applying a linear regression over a minimum of the last three logarithmically transformed data points, allowing a fit with residual square R^2 value of ≥ 0.7. The following parameters are reported: C_{max} (maximum observed plasma concentration), t_{max} (time to maximum observed plasma concentration), AUC_{last} (area under the plasma concentration versus time curve up to the last measured concentration), AUC_{inf} (area under the plasma concentration versus time curve extrapolated to infinity), $t_{1/2}$ (apparent terminal half-life).

For the evaluation of the effect of the interacting drug on the pharmacokinetic parameters of basimglurant an analysis of variance (ANOVA) model was used with the fixed factor treatment and the random factor subject to compare the Test (basimglurant in combination with interacting drug) and Reference (basimglurant administered alone) treatments for $AUC_{0\text{-}last}$ and C_{max} of basimglurant.

Results

Compound Structure and Overall Metabolism

Basimglurant is a weakly basic low molecular weight small molecule drug substance (Jaeschke et al., 2015) which exhibits high permeability and moderate lipophilicity. Metabolism of basimglurant proceeds via oxidation, with no direct conjugation or

JPET Fast Forward. Published on November 7, 2016 as DOI: 10.1124/jpet.116.237214
This article has not been copyedited and formatted. The final version may differ from this version.

hydrolysis metabolites formed. Hydroxylated metabolites are substrates for O-glucuronidation or further oxidation (Figure 1). In a human ADME study, oral bioavailability ranged from 46% to 78% and half-life ranged from 11 to 121 hours, dependent upon the extent of first-pass and systemic metabolism, respectively (Guerini et al., 2016). Absorbed basimglurant was excreted in the form of phase I and subsequent phase II metabolites with essentially no excretion of unchanged parent material.

Enzymology

Basimglurant is metabolized in vitro via hydroxylation of the methyl groups, leading to mono- and di-hydroxylated products as well as further oxidation and glucuronidation of these primary metabolites. The same pattern of metabolism was seen in the human mass balance study (Guerini et al., 2016). The key metabolic step related to the clearance of basimglurant is a methyl hydroxylation resulting in metabolite M1 generation, indicated in Figure 1. M1 is efficiently glucuronidated by UGT1A9 with UGTs 1A3, 1A7, 2B7 and 2B17 also capable of this conjugation reaction (Supplementary Table 3).

CYP Phenotyping: 12 recombinantly expressed individual CYP isoforms were tested for their capability to oxidize basimglurant. CYPs 1A1, 1A2, 2C19, 3A4 and 3A5 were all active in basimglurant metabolism (Supplementary Table 4) and generated metabolite M1 as the main product.

Enzyme Kinetics: Substrate saturation experiments were performed using recombinantly expressed CYPs 1A1, 1A2, 2C19, 3A4 and 3A5 as well as HLM. Plots of the enzyme kinetics can be seen in Figure 2 with the Eadie-Hoftsee plots of the respective kinetics data shown as insets. The form of the kinetics was enzyme-dependent: CYP1A2

JPET Fast Forward. Published on November 7, 2016 as DOI: 10.1124/jpet.116.237214
This article has not been copyedited and formatted. The final version may differ from this version.

exhibited Michaelis-Menten hyperbolic kinetics, CYP1A1 and CYP2C19 followed substrate inhibition kinetics and CYP3A4 and CYP3A5 displayed sigmoidal kinetics. Very similar K_M or S_{50} values were obtained for CYPs 1A1 (4 µM), 1A2 (7 µM), 3A4 (5 µM) and 3A5 (Table 1). The K_M estimate for CYP2C19 was higher (48 µM). Human liver microsomal kinetics were also sigmoidal in form, with an S_{50} of 25 µM estimated. The reason for the difference in S_{50} or K_M values between the individual CYPs and HLM is not known, but may arise from differential protein binding effects, the influence of cytochrome b5 (not present in the individual CYP *E*. coli membrane preparations) or a combination of the two.

Chemical inhibition experiments: when 25 µM basimglurant (S_{50} concentration from HLM kinetics) was incubated with 1 µM ketoconazole, a selective CYP3A4/5 inhibitor, 89% inhibition of metabolism was observed. In contrast, 0.2 µM α-naphthoflavone and 2 µM benzylphenobarbital, selective inhibitors of CYP1A2 and CYP2C19 enzymes, resulted in 17% and <3% inhibition, respectively. The marker reactions tacrine 1-hydroxylase (CYP1A), *S*-mephenytoin 4'-hydroxylase and testosterone 6β-hydroxylase demonstrated the effectiveness and selectivity of the chemical inhibitors (Figure 3; *S*-mephenytoin data not shown). When a low concentration (1 µM) of basimglurant was tested, the effect of the chemical inhibitors was quite different: ketoconazole now inhibited only 27% of metabolism whereas α-naphthoflavone inhibited 69%. These data indicated that the fraction of metabolism catalyzed by the CYP1A2 and CYP3A4/5 changed with basimglurant concentration. To investigate the effect further, an additional in vitro study was performed in which a wide range of basimglurant concentrations were tested. Figure 4 shows how the in vitro kinetics of basimglurant hydroxylation differed in the presence of the selective chemical inhibitors. In the presence of ketoconazole a dramatic reduction in M1 generation was observed at concentrations ranging from 0.8 µM to 25 µM. The

JPET Fast Forward. Published on November 7, 2016 as DOI: 10.1124/jpet.116.237214
This article has not been copyedited and formatted. The final version may differ from this version.

form of the kinetics was transformed from sigmoidal to essentially Michaelis-Menten. However, at the lowest basimglurant concentrations studied, ketoconazole exhibited little inhibition effect. In the presence of α-naphthoflavone the sigmoidal HLM kinetics were largely unaffected over most of the concentrations studied, with only a small reduction in M1 generation rates at concentrations of 3 to 25 µM. However, in the low concentration range (0.8 – 3 µM) a dramatic percentage inhibition effect was observed. At concentrations of 1 µM basimglurant and below, α-naphthoflavone inhibition indicated that CYP1A2 contributed >50% and CYP3A4/5 ~30% of basimglurant metabolism by HLM (Figure 4).

Clinical Findings

Results of clinical studies are shown in Figure 5 with each combination of basimglurant alone and in presence of the interacting drug. Pharmacokinetic parameters from the studies are shown in Table 2.

Ketoconazole DDI study:

When given by itself at 0.25 mg, mean C_{max} and $AUC_{0\text{-}312h}$ values were 1.19 ng/mL and 29.0 hr*ng/mL, respectively. In presence of steady state concentrations of ketoconazole (after multiple daily doses of 400 mg QD), mean C_{max} and $AUC_{0\text{-}312h}$ values of basimglurant were 1.20 ng/mL and 35.9 hr*ng/mL, respectively. Thus, when ketoconazole was co-administered with basimglurant, the C_{max} of basimglurant was not affected (estimated C_{max} ratio = 103% with a 90% CI of 94-113%) but $AUC_{0\text{-}312h}$ was slightly increased (estimated exposure ratio = 124% with 90% CI of 115-134%). Mean plasma ketoconazole C_{max} and $AUC_{0\text{-}24h}$ values were 9.11 µg/mL and 92.3 hr*µg/mL,

JPET Fast Forward. Published on November 7, 2016 as DOI: 10.1124/jpet.116.237214
This article has not been copyedited and formatted. The final version may differ from this version.

respectively. In the presence of basimglurant, ketoconazole mean C_{max} and $AUC_{0\text{-}24h}$ values were 9.73 µg/mL and 95.8 hr*µg/mL, respectively. Basimglurant is therefore seen to have a low first pass extraction and ketoconazole can be considered a weak inhibitor of basimglurant clearance, the majority of the effect exhibited in inhibition of systemic clearance.

Carbamazepine DDI study:

When given by itself as a 0.5 mg single dose, mean C_{max} and $AUC_{0\text{-}312h}$ values were 1.71 ng/mL, and 45.2 ng*h/mL. In presence of steady state concentrations of carbamazepine after multiple doses (400 mg BID), mean C_{max} and $AUC_{0\text{-}312h}$ values of basimglurant were 1.34 ng/mL and 28.5 ng*h/mL, respectively. Thus, when carbamazepine was co-administered with basimglurant, both C_{max} was decreased (estimated ratio 0.78 (90% CI: 0.70-0.87), and $AUC_{0\text{-}312h}$ of basimglurant was decreased (estimated ratio = 0.63 (90% CI: 0.54-0.73). Concentrations of carbamazepine remained unaffected in the presence of basmiglurant. Geometric mean C_{max} and $AUC_{0\text{-}12h}$ values of carbamazepine when given alone were 9.36 µg/mL and 101.7 µg*h/mL, respectively. In combination, mean C_{max} and $AUC_{0\text{-}12h}$ values were 9.28 µg/mL and 101.9 µg*h/mL. It can be concluded that carbamazepine had an effect on basimglurant pharmacokinetic profile, with approximately a reduction of C_{max} by 22% and $AUC_{0\text{-}312h}$ by 37%.

Fluvoxamine DDI study:

When given by itself as a 0.2 mg single dose, mean C_{max} and $AUC_{0\text{-}312h}$ values were 0.629 ng/mL and 17.3 ng*h/mL. In the presence of steady state concentrations of fluvoxamine after multiple doses (100 mg QD in the evening), mean C_{max} and $AUC_{0\text{-}312h}$ values of basimglurant were 0.699 ng/mL and 27.8 ng*h/mL, respectively. Thus, when fluvoxamine was co-administered with basimglurant, the C_{max} of basimglurant was not

JPET Fast Forward. Published on November 7, 2016 as DOI: 10.1124/jpet.116.237214
This article has not been copyedited and formatted. The final version may differ from this version.

affected (estimated ratio = 1.11 with 90% CI of 0.98-1.26), but $AUC_{0\text{-}312h}$ was increased (estimated ratio = 1.60 with 90% CI: 1.40-1.84). Hence, fluvoxamine had no major effect on basimglurant plasma peak level, but had an effect on plasma basimglurant exposure, resulting in a ~1.6-fold increase in $AUC_{0\text{-}312h}$. Statistical analysis on the C_{trough} values of fluvoxamine indicated a small impact (20%) of basimglurant on the PK of fluvoxamine (geometric mean [90% CI] C_{trough} alone = 35.4 [25.8 - 48.6] ng/mL, and in combination = 42.4 [30.8 - 58.2] ng/mL, ratio = 1.20 [1.12 - 1.28]. It can be concluded that fluvoxamine at steady-state and administered during a large part of basimglurant elimination phase, had a moderate inhibitory effect on basimglurant clearance.

In each of the studies, concentrations of the interacting drugs appeared to be at steady state, at least by visual examination, and were not impacted at all or only to a small extent by presence of basimglurant indicating a low potential of basimglurant to affect the interacting drug pharmacokinetics.

JPET Fast Forward. Published on November 7, 2016 as DOI: 10.1124/jpet.116.237214
This article has not been copyedited and formatted. The final version may differ from this version.

Discussion

Enzyme phenotyping data, conducted using a combination of recombinantly expressed individual enzymes and CYP-selective chemical inhibitors, showed that CYPs 1A1, 1A2, 2C19, 3A4 and 3A5 were capable of basimglurant metabolism, with the hydroxylated metabolite M1 the main product generated. Enzyme kinetics experiments showed that CYP1A2 and CYP3A4/5 had very similar K_M or S_{50} values, giving no obvious kinetic basis for concentration-dependent changes in $f_{m(CYP\ isoform)}$. Chemical inhibitor studies conducted using pooled human liver microsomes at the HLM S_{50} concentration of 25 µM indicated that basimglurant metabolism was principally mediated by CYP3A4/5 with only a minor contribution of CYP1A2. These results were followed up with a clinical drug-drug interaction study to examine the effect of multiple dose ketoconazole on basimglurant pharmacokinetics in healthy subjects. Only a 1.24-fold mean increase in basimglurant AUC and essentially no increase in C_{max} was observed when basimglurant was coadministered with ketoconazole. In contrast, for sensitive substrates of CYP3A4/5 such as the high clearance drug midazolam, and the low clearance drug alprazolam, exposures have been reported to be increased 8-15-fold and 3-fold, respectively, on coadministration with ketoconazole (Olkkola et al., 1994; Lam et al., 2003; Boulenc et al., 2016). A clinical DDI study using the CYP3A4/5 inducer carbamazepine resulted in an average basimglurant AUC decrease of 37% and a C_{max} decrease of 22%. Again this contrasted with reported carbamazepine interaction study data for CYP3A4/5 substrates such as simvastatin (75% reduction in AUC (Ucar et al., 2004)) and alprazolam (2.4-fold increase in clearance (Furukori et al., 1998)). These results indicated that whilst basimglurant metabolism could be induced somewhat by carbamazepine and that CYP3A4/5 were likely to play a role in clearance, they did not represent the main

elimination pathway, especially when one considers that carbamazepine is also capable of weak CYP1A2 induction (Sugiyama et al., 2016).

In a human mass balance study, where basimglurant was administered orally, no unchanged drug substance was recovered in either the feces or urine samples, indicating essentially complete absorption and metabolism. Two potential reasons for the lack of CYP3A4/5 dominance in metabolic clearance were therefore investigated. (1) Potential for extrahepatic metabolism by enzymes other than CYP3A4/5: In vitro experiments performed using pooled human kidney and lung microsomes obtained from commercial sources established that the rates of basimglurant oxidation were >250-fold lower, per milligram of microsomal protein, for these tissues compared with liver (data not shown). Although not all possible human tissues were explored, these data did not indicate a strong possibility for extrahepatic clearance of basimglurant. (2) Influence of basimglurant concentration: One feature of the human drug-drug interaction studies which differed significantly from the initial in vitro experiments was the basimglurant concentration. Plasma C_{max} concentrations were in the range 0.5 – 2 ng/mL (1.5 – 6 nM), more than 10,000 times lower than in the initial in vitro studies. Additional inhibition studies were performed using 1 µM basimglurant as substrate concentration. [Although this was still a substantially higher concentration than in vivo, it was the lowest effectively testable concentration given the low rate of metabolism and sensitivity of M1 quantification.] A very different pattern of inhibitor sensitivity was obtained when 1 µM basimglurant was used as substrate compared with 25 µM (Figure 3). This strongly indicated that CYP1A2 was more important for metabolism than CYP3A4/5 at low basimglurant concentrations. Further inhibition studies performed over a wide range of concentrations confirmed that there was a steady change in the fractional contributions of CYP3A4/5 and CYP1A2 to basimglurant metabolism with change in basimglurant

JPET Fast Forward. Published on November 7, 2016 as DOI: 10.1124/jpet.116.237214
This article has not been copyedited and formatted. The final version may differ from this version.

concentration (Figure 4). Rough estimates of approximately 30% CYP3A4/5 and 70% CYP1A2 contribution at low concentrations were made from these additional inhibition experiments.

A further in vivo DDI study was performed using fluvoxamine as an inhibitor of CYP1A2. Although fluvoxamine may inhibit other CYP enzymes, the inhibition effect of fluvoxamine on basimglurant metabolism should selectively be mediated via CYP1A2, as CYP2C19 did not significantly contribute to the metabolism of basimglurant in vitro and the concentrations of fluvoxamine attained were too low to cause inhibition of CYP3A4. Coadministration of fluvoxamine resulted in a 1.6-fold increase in basimglurant AUC and a 1.1-fold increase in C_{max} (Figure 5, Table 2). These interaction effects are consistent with CYP1A2 contributing ~70% to basimglurant metabolism, given the relatively short half-life of fluvoxamine, the extent of CYP1A2 inhibition attained clinically and the low first-pass extraction of basimglurant. A physiologically-based human PK model of basimglurant has been developed which considers hepatic metabolism through CYPs 1A2 and 3A4 enzymes as the exclusive elimination pathways with metabolic contributions defined as 30% and 70% for CYPs 3A4/5 and 1A2, respectively. This model accurately predicted DDI with ketoconazole (observed vs. predicted geometric mean AUC ratios: 1.24 vs. 1.49) and fluvoxamine (observed vs. predicted geometric mean AUC ratios: 1.60 vs. 1.78), demonstrating consistency in in vitro and in vivo metabolic fractions of both CYPs 3A4 and 1A2 enzymes (manuscript in preparation).

Cases where more than one metabolic enzyme contributes to the metabolism of a drug are frequently encountered and mitigate against high exposure differences due to single enzyme polymorphisms or drug-drug interactions. Where the metabolic enzymes have quite different K_M values, one enzyme may become saturated as the drug concentration increases, changing the relative enzyme contributions to overall metabolism. This may

be seen clearly in the biphasic kinetics exhibited by such drugs, for instance CYP2D6- and CYP3A4-mediated dextromethorphan O-demethylation (von Moltke et al., 1998), CYP2C19 and CYP3A4 mediated diazepam oxidation (Andersson et al., 1994; Galetin et al., 2004) and RO5263397 glucuronidation (Fowler et al., 2015). Attention may then be focused on the low K_M isoform as the likely main contributor to metabolism in vivo. For basimglurant there was no saturation of metabolic enzymes, nor was there significant difference in the K_M (or S_{50}) values for CYP1A2 and CYP3A4/5 . However, the substrate-saturation kinetics exhibited different profiles for the various CYP isoforms involved (Figure 2, Table 1). The HLM kinetics are dominated by the CYP3A4/5 component in the 5-50 µM concentration range over which most of the data for the S_{50} determination were obtained. Indeed, the Eadie-Hoftsee plot did not indicate biphasic kinetic character and the relevance of the CYP1A2 component was only revealed by inhibition studies using low concentrations of basimglurant. Kinetics are sigmoidal for both CYPs 3A4 and 3A5 compared with hyperbolic kinetics for CYP1A2. The superimposition of these two distinct kinetic forms can be seen in the human liver microsomal kinetics when determined in the presence of selective CYP3A4/5 or CYP1A2 inhibitors (Figure 4). As the substrate concentration drops, the rate of metabolism by CYP1A2 decreases proportionately, since substrate concentration is $<<K_M$ and CYP1A2 follows Michaelis-Menten kinetics. However, for CYP3A4/5 , the rate of turnover decreases more than proportionately with decreasing substrate concentration due to the sigmoidal kinetics. This combination of differential enzyme kinetic forms explains the in vitro concentration dependence of CYP involvement in basimglurant metabolism.

Many compounds display sigmoidal kinetics in vitro but there are few reports of the relevance of this to the in vivo situation. In principle, for compounds whose metabolism follows sigmoidal kinetics, suprapropotional exposure should be observed in dose

JPET Fast Forward. Published on November 7, 2016 as DOI: 10.1124/jpet.116.237214
This article has not been copyedited and formatted. The final version may differ from this version.

escalation studies and enhanced clearance should be seen when administered with allosteric enhancers. However, evidence for translation of these kinetic phenomena into clear pharmacokinetic effects remains scant. In one example of a clinical study specifically performed to explore such effects, dapsone (an enhancer of CYP2C9-mediated flurbiprofen metabolism in vitro) was co-administered with flurbiprofen to healthy volunteers (Hutzler et al., 2001). Despite multiple dosing of dapsone, which resulted in plasma concentrations of ~11 μM, only marginal enhancement of flurbiprofen hydroxylation and clearance could be detected, likely due to high protein binding limiting the free dapsone concentrations as well as the clearance of flurbiprofen via other pathways (Davies, 1995; Mano et al., 2007).

Confounding factors which reduce the chance of observing the potential relevance of sigmoidal kinetics studies in man include the very high concentrations required for the sigmoidal nature of the kinetics to be demonstrated, compared to the plasma, liver and intestinal concentrations and the scarcity of multiple dose pharmacokinetic data available from the same individual (which might help in overcoming problems associated with inter-individual variability in clearance). In addition, pharmacokinetic phenomena such as solubility and absorption limitation of exposure at higher doses may have been assigned to explain any suprapproportional exposure increase with increasing dose. In a similar manner, reduced systemic clearance at low circulating concentrations of compounds such as basimglurant may be missed either due to analytical sensitivity limitations or assigned to slow drug release from a high affinity binding compartment, rather than being associated with decreased metabolic clearance at low concentrations.

In conclusion, basimglurant is metabolized by both CYP1A2 and CYP3A4/5 isoforms resulting in a low liability as a subject (victim) of metabolism-based drug-drug interactions. The in vitro enzymology data explain the in vivo situation well when low

concentrations of basimglurant are used for the studies. Where higher concentrations were tested, the combination of differential kinetics resulted in an estimation of fraction metabolized which was not relevant for the in vivo situation. This study highlights the importance of enzyme kinetics in the understanding and prediction of fraction metabolized, emphasizes the need for in vitro testing to be performed under conditions from which the data can be extrapolated to the in vivo situation and highlights the importance of close communication between drug metabolism, modelling and simulation and clinical pharmacology disciplines in order to understand the complexities of drug-drug interactions.

Acknowledgements

The authors gratefully acknowledge the technical assistance of Paul Schmid in performing the initial CYP incubations and the laboratory of Dr Thomas Hartung where radiolabelled basimglurant was prepared. The help of Kevin Duffy in planning the fluvoxamine interaction study was also greatly appreciated.

Authorship Contributions:

Experimental design, experimental work and data processing: Fowler, Guerini, Qiu, Greig and Mallalieu

Data interpretation: Fowler, Guerini, Cleary, Parrot, Greig and Mallalieu.

Writing of the manuscript: Fowler and Mallalieu with assistance from the other authors

Conflict of interest/Disclosure:

All authors are employees of F. Hoffmann-La Roche Ltd. and have no conflicts of interest to disclose.

This work was supported by F. Hoffmann-La Roche Ltd.

JPET Fast Forward. Published on November 7, 2016 as DOI: 10.1124/jpet.116.237214
This article has not been copyedited and formatted. The final version may differ from this version.

References

Andersson T, Miners JO, Veronese ME and Birkett DJ (1994) Diazepam metabolism by human liver microsomes is mediated by both S-mephenytoin hydroxylase and CYP3A isoforms. *British journal of clinical pharmacology* **38**:131-137.

Atkins WM (2005) Non-Michaelis-Menten kinetics in cytochrome P450-catalyzed reactions. *Annual review of pharmacology and toxicology* **45**:291-310.

Berman RM, Narasimhan M, Sanacora G, Miano AP, Hoffman RE, Hu XS, Charney DS and Boutros NN (2000) A randomized clinical trial of repetitive transcranial magnetic stimulation in the treatment of major depression. *Biol Psychiatry* **47**:332-337.

Boulenc X, Nicolas O, Hermabessiere S, Zobouyan I, Martin V, Donazzolo Y and Ollier C (2016) CYP3A4-based drug-drug interaction: CYP3A4 substrates' pharmacokinetic properties and ketoconazole dose regimen effect. *European journal of drug metabolism and pharmacokinetics* **41**:45-54.

Chaki S, Ago Y, Palucha-Paniewiera A, Matrisciano F and Pilc A (2013) mGlu2/3 and mGlu5 receptors: potential targets for novel antidepressants. *Neuropharmacology* **66**:40-52.

Connolly KR and Thase ME (2012) Emerging drugs for major depressive disorder. *Expert Opin Emerg Drugs* **17**:105-126.

Davies NM (1995) Clinical pharmacokinetics of flurbiprofen and its enantiomers. *Clinical pharmacokinetics* **28**:100-114.

Duman RS, Li N, Liu RJ, Duric V and Aghajanian G (2012) Signaling pathways underlying the rapid antidepressant actions of ketamine. *Neuropharmacology* **62**:35-41.

EMA (2012) Guideline on the investigation of drug interactions. *Committee for Human Medicinal Products (CHMP)*.

FDA (2012) Drug interaction studies - study design, data analysis, implications for dosing, and labeling recommendations, in.

Ferrari AJ, Charlson FJ, Norman RE, Patten SB, Freedman G, Murray CJL, Vos T and Whiteford HA (2013) Burden of Depressive Disorders by Country, Sex, Age, and Year: Findings from the Global Burden of Disease Study 2010. *Plos Med* **10**.

Fowler S, Kletzl H, Finel M, Manevski N, Schmid P, Tuerck D, Norcross RD, Hoener MC, Spleiss O and Iglesias VA (2015) A UGT2B10 splicing polymorphism common in african populations may greatly increase drug exposure. *The Journal of pharmacology and experimental therapeutics* **352**:358-367.

Fowler SM, Taylor JM, Friedberg T, Wolf CR and Riley RJ (2002) CYP3A4 active site volume modification by mutagenesis of leucine 211. *Drug metabolism and disposition: the biological fate of chemicals* **30**:452-456.

Furukori H, Otani K, Yasui N, Kondo T, Kaneko S, Shimoyama R, Ohkubo T, Nagasaki T and Sugawara K (1998) Effect of carbamazepine on the single oral dose pharmacokinetics of alprazolam. *Neuropsychopharmacology* **18**:364-369.

Galetin A, Brown C, Hallifax D, Ito K and Houston JB (2004) Utility of recombinant enzyme kinetics in prediction of human clearance: impact of variability,

CYP3A5, and CYP2C19 on CYP3A4 probe substrates. *Drug metabolism and disposition: the biological fate of chemicals* **32**:1411-1420.

Guerini E, Schadt S, Greig G, Haas R, Husser C, Zell M, Funk C, Hartung T, Gloge A and Mallalieu NL (2016) A double-tracer technique to characterize absorption, distribution, metabolism and excretion (ADME) of [C]-basimglurant and absolute bioavailability after oral administration and concomitant intravenous microdose administration of [C]-labeled basimglurant in humans. *Xenobiotica; the fate of foreign compounds in biological systems*:1-10.

Gufford BT, Lu JB, Metzger IF, Jones DR and Desta Z (2016) Stereoselective Glucuronidation of Bupropion Metabolites In Vitro and In Vivo. *Drug metabolism and disposition: the biological fate of chemicals* **44**:544-553.

Huang C, Chen Y, Zhou T and Chen G (2009) Sulfation of dietary flavonoids by human sulfotransferases. *Xenobiotica; the fate of foreign compounds in biological systems* **39**:312-322.

Hutzler JM, Frye RF, Korzekwa KR, Branch RA, Huang SM and Tracy TS (2001) Minimal in vivo activation of CYP2C9-mediated flurbiprofen metabolism by dapsone. *Eur J Pharm Sci* **14**:47-52.

Hutzler JM and Tracy TS (2002) Atypical kinetic profiles in drug metabolism reactions. *Drug metabolism and disposition: the biological fate of chemicals* **30**:355-362.

Jaeschke G, Kolczewski S, Spooren W, Vieira E, Bitter-Stoll N, Boissin P, Borroni E, Buttelmann B, Ceccarelli S, Clemann N, David B, Funk C, Guba W, Harrison A, Hartung T, Honer M, Huwyler J, Kuratli M, Niederhauser U, Pahler A, Peters JU, Petersen A, Prinssen E, Ricci A, Rueher D, Rueher M, Schneider M, Spurr P, Stoll T, Tannler D, Wichmann J, Porter RH, Wettstein JG and Lindemann L (2015) Metabotropic glutamate receptor 5 negative allosteric modulators: discovery of 2-chloro-4-[1-(4-fluorophenyl)-2,5-dimethyl-1H-imidazol-4-ylethynyl]pyridine (basimglurant, RO4917523), a promising novel medicine for psychiatric diseases. *J Med Chem* **58**:1358-1371.

Krystal JH, Sanacora G and Duman RS (2013) Rapid-acting glutamatergic antidepressants: the path to ketamine and beyond. *Biol Psychiatry* **73**:1133-1141.

Lam YW, Alfaro CL, Ereshefsky L and Miller M (2003) Pharmacokinetic and pharmacodynamic interactions of oral midazolam with ketoconazole, fluoxetine, fluvoxamine, and nefazodone. *Journal of clinical pharmacology* **43**:1274-1282.

Licznerski P and Duman RS (2013) Remodeling of axo-spinous synapses in the pathophysiology and treatment of depression. *Neuroscience* **251**:33-50.

Lindemann L, Porter RH, Scharf SH, Kuennecke B, Bruns A, von Kienlin M, Harrison AC, Paehler A, Funk C, Gloge A, Schneider M, Parrott NJ, Polonchuk L, Niederhauser U, Morairty SR, Kilduff TS, Vieira E, Kolczewski S, Wichmann J, Hartung T, Honer M, Borroni E, Moreau JL, Prinssen E, Spooren W, Wettstein JG and Jaeschke G (2015) Pharmacology of basimglurant (RO4917523, RG7090), a unique metabotropic glutamate receptor 5 negative allosteric modulator in clinical development for depression. *J Pharmacol Exp Ther* **353**:213-233.

Manji HK, Quiroz JA, Sporn J, Payne JL, Denicoff K, N AG, Zarate CA, Jr. and Charney DS (2003) Enhancing neuronal plasticity and cellular resilience to develop novel, improved therapeutics for difficult-to-treat depression. *Biol Psychiatry* **53**:707-742.

Mano Y, Usui T and Kamimura H (2007) Predominant contribution of UDP-glucuronosyltransferase 2B7 in the glucuronidation of racemic flurbiprofen in the human liver. *Drug metabolism and disposition: the biological fate of chemicals* **35**:1182-1187.

Olkkola KT, Backman JT and Neuvonen PJ (1994) Midazolam should be avoided in patients receiving the systemic antimycotics ketoconazole or itraconazole. *Clinical pharmacology and therapeutics* **55**:481-485.

Quiroz JA CG, Drevets W, Manji HK. (2012) *Translational Neuroscience: Applications in Neurology, Psychiatry, and Neurodevelopmental Disorders*. Cambridge University Press

Quiroz JA, Tamburri P, Deptula D, Banken L, Beyer U, Rabbia M, Parkar N, Fontoura P and Santarelli L (2016) Efficacy and Safety of Basimglurant as Adjunctive Therapy for Major Depression: A Randomized Clinical Trial. *JAMA Psychiatry* **73**:675-684.

Rush AJ, Trivedi MH, Wisniewski SR, Stewart JW, Nierenberg AA, Thase ME, Ritz L, Biggs MM, Warden D, Luther JF, Shores-Wilson K, Niederehe G and Fava M (2006) Bupropion-SR, sertraline, or venlafaxine-XR after failure of SSRIs for depression. *N Engl J Med* **354**:1231-1242.

Shou M, Grogan J, Mancewicz JA, Krausz KW, Gonzalez FJ, Gelboin HV and Korzekwa KR (1994) Activation of CYP3A4: evidence for the simultaneous binding of two substrates in a cytochrome P450 active site. *Biochemistry* **33**:6450-6455.

Shou M, Lin Y, Lu P, Tang C, Mei Q, Cui D, Tang W, Ngui JS, Lin CC, Singh R, Wong BK, Yergey JA, Lin JH, Pearson PG, Baillie TA, Rodrigues AD and Rushmore TH (2001) Enzyme kinetics of cytochrome P450-mediated reactions. *Current drug metabolism* **2**:17-36.

Sugiyama I, Murayama N, Kuroki A, Kota J, Iwano S, Yamazaki H and Hirota T (2016) Evaluation of cytochrome P450 inductions by anti-epileptic drug oxcarbazepine, 10-hydroxyoxcarbazepine, and carbamazepine using human hepatocytes and HepaRG cells. *Xenobiotica; the fate of foreign compounds in biological systems* **46**:765-774.

Ucar M, Neuvonen M, Luurila H, Dahlqvist R, Neuvonen PJ and Mjorndal T (2004) Carbamazepine markedly reduces serum concentrations of simvastatin and simvastatin acid. *European journal of clinical pharmacology* **59**:879-882.

Uchaipichat V, Mackenzie PI, Guo XH, Gardner-Stephen D, Galetin A, Houston JB and Miners JO (2004) Human udp-glucuronosyltransferases: isoform selectivity and kinetics of 4-methylumbelliferone and 1-naphthol glucuronidation, effects of organic solvents, and inhibition by diclofenac and probenecid. *Drug metabolism and disposition: the biological fate of chemicals* **32**:413-423.

von Moltke LL, Greenblatt DJ, Grassi JM, Granda BW, Venkatakrishnan K, Schmider J, Harmatz JS and Shader RI (1998) Multiple human cytochromes contribute to biotransformation of dextromethorphan in-vitro: role of CYP2C9, CYP2C19,

CYP2D6, and CYP3A. *The Journal of pharmacy and pharmacology* **50**:997-1004.

Williams PA, Cosme J, Vinkovic DM, Ward A, Angove HC, Day PJ, Vonrhein C, Tickle IJ and Jhoti H (2004) Crystal structures of human cytochrome P450 3A4 bound to metyrapone and progesterone. *Science (New York, NY* **305**:683-686.

Wu B (2011) Substrate inhibition kinetics in drug metabolism reactions. *Drug metabolism reviews* **43**:440-456.

Yano JK, Wester MR, Schoch GA, Griffin KJ, Stout CD and Johnson EF (2004) The structure of human microsomal cytochrome P450 3A4 determined by X-ray crystallography to 2.05-A resolution. *The Journal of biological chemistry* **279**:38091-38094.

Zarate CA, Jr., Singh JB, Carlson PJ, Brutsche NE, Ameli R, Luckenbaugh DA, Charney DS and Manji HK (2006a) A randomized trial of an N-methyl-D-aspartate antagonist in treatment-resistant major depression. *Arch Gen Psychiatry* **63**:856-864.

Zarate CA, Jr., Singh JB, Quiroz JA, De Jesus G, Denicoff KK, Luckenbaugh DA, Manji HK and Charney DS (2006b) A double-blind, placebo-controlled study of memantine in the treatment of major depression. *Am J Psychiatry* **163**:153-155.

Zarate CA, Jr. and Tohen M (2004) Double-blind comparison of the continued use of antipsychotic treatment versus its discontinuation in remitted manic patients. *Am J Psychiatry* **161**:169-171.

Zhang H, Davis CD, Sinz MW and Rodrigues AD (2007) Cytochrome P450 reaction-phenotyping: an industrial perspective. *Expert opinion on drug metabolism & toxicology* **3**:667-687.

Zientek MA and Youdim K (2015) Reaction phenotyping: advances in the experimental strategies used to characterize the contribution of drug-metabolizing enzymes. *Drug metabolism and disposition: the biological fate of chemicals* **43**:163-181.

JPET Fast Forward. Published on November 7, 2016 as DOI: 10.1124/jpet.116.237214
This article has not been copyedited and formatted. The final version may differ from this version.

Figure Legends

Figure 1: Human Metabolism of Basimglurant

Major pathways marked with bold arrows, minor pathways marked with faint arrows. Conversion of basimglurant to metabolite M1 is the rate determining step in basimglurant clearance.

Figure 2: Substrate-Saturation Kinetics of Basimglurant Hydroxylation by Individual Recombinantly Expressed CYP Isoforms and Pooled Human Liver Microsomes.

Substrate-saturation kinetics of M1 formation from basimglurant by human liver microsomes and CYPs 1A1, 1A2, 2C19, 3A4 and 3A5. A Michaelis-Menten equation was fitted to the CYP1A2 data, a substrate inhibition equation was fitted to CYP1A1 and CYP2C19 data and a sigmoidal (Hill) equation was fitted to CYP3A4, CYP3A5 and HLM data. Inset figures show Eadie-Hoftsee plots of M1 formation rate against rate/substrate concentration for each of the kinetics profiles.

Figure 3: Effect of CYP-Selective Chemical Inhibitors on Basimglurant Hydroxylation by Pooled Human Liver Microsomes

Histograms showing the effect of 0.2 μM α-naphthoflavone (ANF, CYP1A2 inhibitor), 2 μM benzylphenobarbital (BPB, CYP2C19 inhibitor), and 1 μM ketoconazole (KET, CYP3A4/5 inhibitor) in relation to with DMSO control (DMSO) on human liver microsomal basimglurant hydroxylation to M1 as well as testosterone 6β-hydroxylation

(CYP3A4/5-mediated) and tacrine 1-hydroxylation (CYP1A2-mediated) activities. p-values of <0.001 were attained for α-naphthoflavone inhibition of basimglurant hydroxylation (1 µM) and for ketoconazole inhibition of basimglurant hydroxylation (both 1 and 25 µM).

Figure 4: Effect of CYP-Selective Chemical Inhibitors on Pooled Human Liver Microsomal Basimglurant Hydroxylation Assessed at Various Basimglurant Concentrations.

Human liver microsomal metabolism of basimglurant, tested at multiple concentrations, to metabolite M1 in the presence of fixed concentrations of CYP-selective chemical inhibitors (or DMSO solvent control). A: Direct plot of M1 generation rate in the presence of 0.2 µM alpha-naphthoflavone and 1 µM ketoconazole against basimglurant concentration. B: Percentage inhibition effect data (DMSO control activity set as 100% activity) plotted as a function of Basimglurant concentration. p-values of <0.001 attained for α-naphthoflavone inhibition of basimglurant hydroxylation at all test concentrations except for 0.78 µM (p=0.003) and 25 µM (p=0.15). p-values of <0.001 were attained for ketoconazole inhibition of basimglurant hydroxylation at all test concentrations.

Figure 5: Effects of Ketoconazole, Carbamazepine and Fluvoxamine on Mean Oral Basimglurant Pharmacokinetics

Mean (SD) plasma concentration profiles of basimglurant when given alone and in the presence of steady state levels of a) 400 mg QD Ketoconazole (KETO) b) 400 mg BID Carbamazepine (CBZ) and c) 100 mg QD Fluvoxamine

JPET Fast Forward. Published on November 7, 2016 as DOI: 10.1124/jpet.116.237214
This article has not been copyedited and formatted. The final version may differ from this version.

Figure 6: Overview of the Effect of Ketoconazole, Carbamazepine and Fluvoxamine on Basimglurant Pharmacokinetics

Forest plot showing an overview of AUC and C_{max} changes for basimglurant in the presence of CYP inhibitors and inducers. Mean interaction values with 90% confidence intervals shown. Dotted lines indicate bioequivalence limits of 0.8 and 1.25.

Table 1: Kinetics of Human Liver Microsomal and CYP Enzyme Mediated Hydroxylation of Basimglurant to Generate Metabolite M1

	Michaelis-Menten Model		Hill Model			Substrate Inhibition Model		
Enzyme	K_M [a]	V_{max} [b]	S_{50} [a]	V_{max} [b]	*n*	K_M [a]	V_{max} [b]	K_i [a]
HLM	-	-	25 ±1	0.37 ±0.01	1.7 ±0.1	-	-	-
CYP1A1	-	-	-	-	-	4.2 ±0.6	25 ±2	110 ±30
CYP1A2	6.8 ±0.4	0.11 ±0.01	-	-	-	-	-	-
CYP2C19	-	-	-	-	-	48 ±10	0.26 ±0.04	23 ±5
CYP3A4	-	-	6.5 ±0.5	0.16 ±0.01	1.8 ±0.2	-	-	-
CYP3A5	-	-	5.2 ±0.2	0.48 ±0.01	1.6 ±0.1	-	-	-

[a] K_M, K_i and S_{50} values in µM.
[b] V_{max} values in pmol equivalents/min/pmol recombinantly expressed CYP, or nmol/min/mg HLM protein.

Table 2: Treatment comparison of basimglurant after administration of basimglurant alone or in combination with multiple doses of various interacting drugs

Parameter (unit)	Reference: Basimglurant Alone[(a)]	Test: Basimglurant administered with interacting drug[(a)]	Test/Reference [(b)]
Ketoconazole [(c)] N=18 (9M/9F)			
$AUC_{0\text{-}312h}$ (ng*h/mL)	**28.91** [24.0, 34.8]	**35.9** [29.9, 43.2]	**1.24** [1.15,1.34]
C_{max} (ng/mL)	**1.17** [1.06, 1.29]	**1.20** [1.09, 1.33]	**1.03** [0.94, 1.13]
Carbamazepine [(d)] N=16 (12M/4F)			
$AUC_{0\text{-}312h}$ (ng*h/mL)	**45.2** [37.1, 55.0]	**28.5** [23.4, 34.7]	**0.630** [0.542, 0.733]
C_{max} (ng/mL)	**1.70** [1.50,1.90]	**1.30** [1.20,1.50]	**0.782** [0.704, 0.869]
Fluvoxamine [(e)] N=16 (12M/4F)			
$AUC_{0\text{-}312h}$ (ng*h/mL)	**17.3** [12.3, 24.4]	**27.8** [19.7, 39.1]	**1.60** [1.40, 1.84]

C_{max} (ng/mL)	**0.629** [0.548, 0.722]	**0.699** [0.609, 0.802]	**1.11** [0.98, 1.26]

a) Geometric least square mean (90% confidence interval (CI));

b) Point estimate (90% CI) for Test/Reference geo ls mean

c) basimglurant single dose 0.25 mg, ketoconazole multiple doses of 400 mg QD;

d) basimglurant single dose 0.5 mg, carbamazepine multiple doses of 400 mg BID;

e) basimglurant single dose 0.2 mg, fluvoxamine multiple doses of 100 mg QD

Figure 1

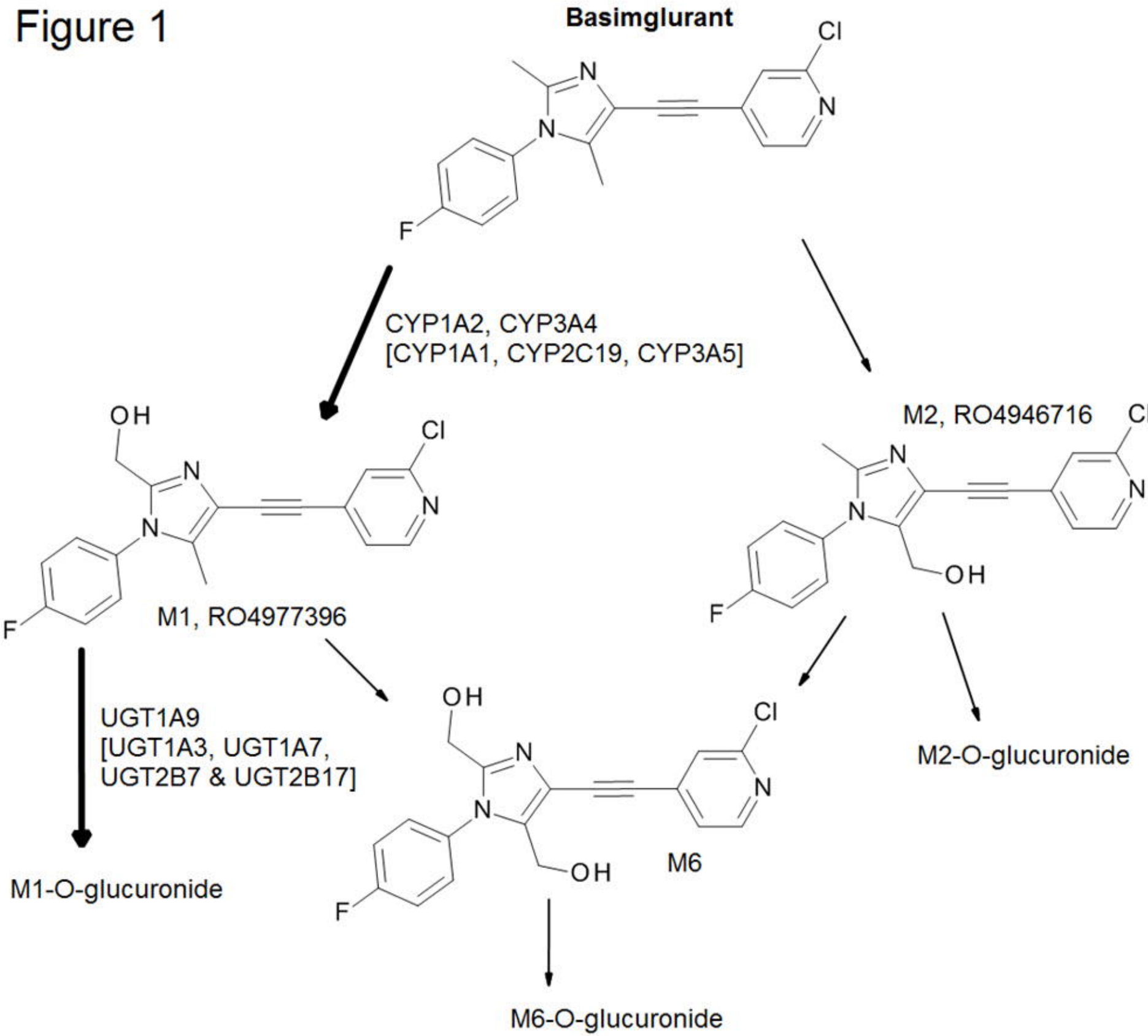
Basimglurant
CYP1A2, CYP3A4
[CYP1A1, CYP2C19, CYP3A5]
M1, RO4977396
M2, RO4946716
UGT1A9
[UGT1A3, UGT1A7,
UGT2B7 & UGT2B17]
M1-O-glucuronide
M2-O-glucuronide
M6
M6-O-glucuronide

Figure 2

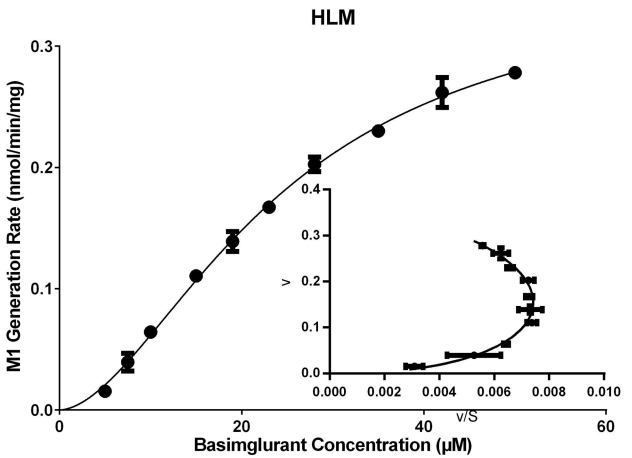
HLM
M1 Generation Rate (nmol/min/mg)
Basimglurant Concentration (μM)
v
v/S

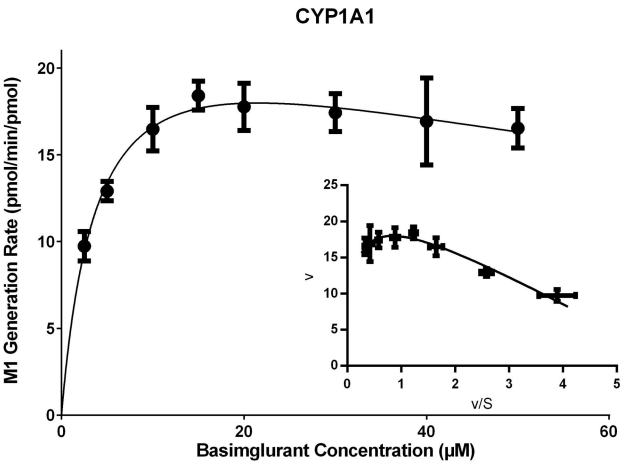
CYP1A1
M1 Generation Rate (pmol/min/pmol)
Basimglurant Concentration (μM)
v
v/S

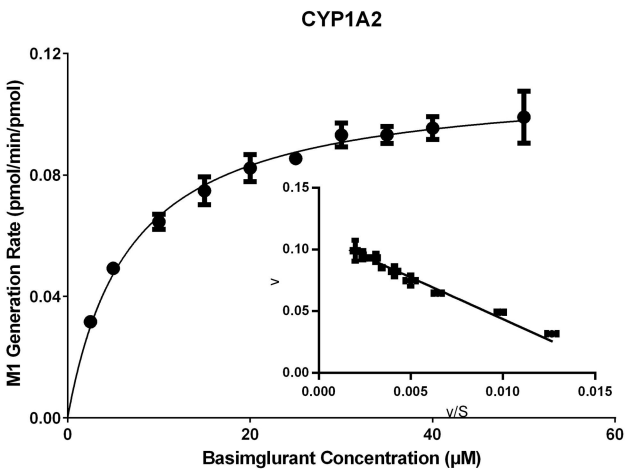
CYP1A2
M1 Generation Rate (pmol/min/pmol)
Basimglurant Concentration (μM)
v
v/S

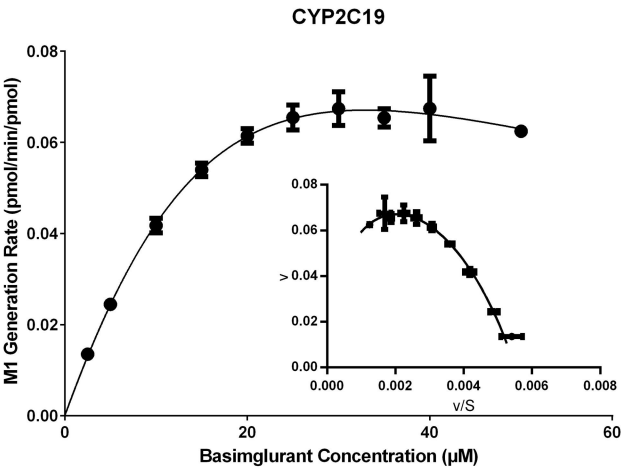
CYP2C19
M1 Generation Rate (pmol/min/pmol)
Basimglurant Concentration (μM)
v
v/S

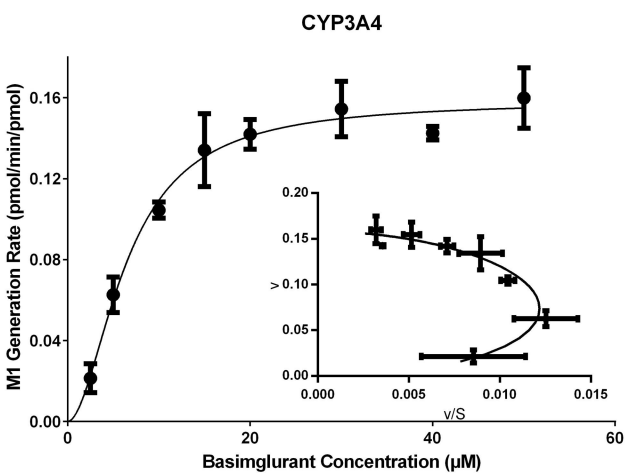
CYP3A4
M1 Generation Rate (pmol/min/pmol)
Basimglurant Concentration (μM)
v
v/S

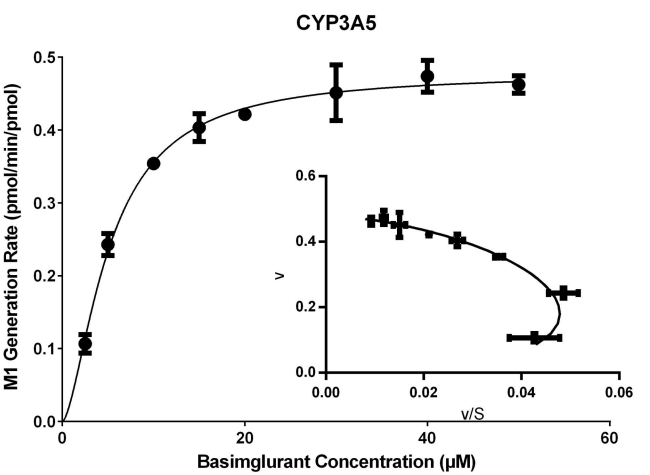
CYP3A5
M1 Generation Rate (pmol/min/pmol)
Basimglurant Concentration (μM)
v
v/S

Figure 3

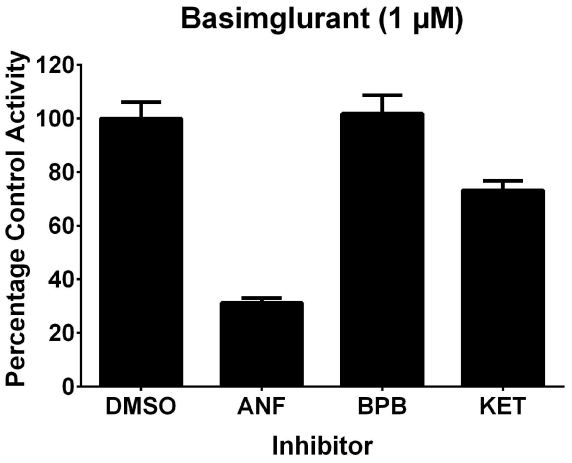
Basimglurant (1 μM)
Percentage Control Activity
120
100
80
60
40
20
0
DMSO
ANF
BPB
KET
Inhibitor

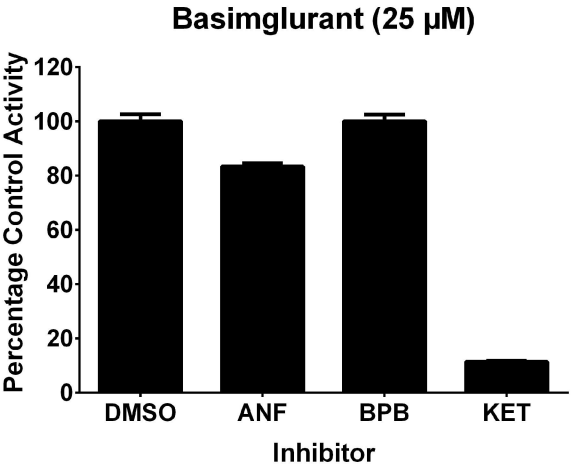
Basimglurant (25 μM)
Percentage Control Activity
120
100
80
60
40
20
0
DMSO
ANF
BPB
KET
Inhibitor

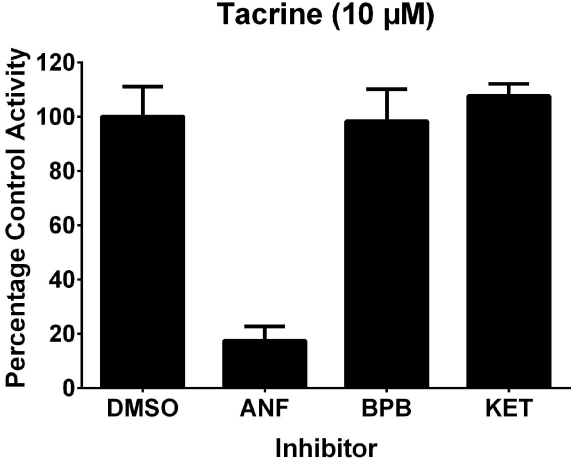
Tacrine (10 μM)
Percentage Control Activity
120
100
80
60
40
20
0
DMSO
ANF
BPB
KET
Inhibitor

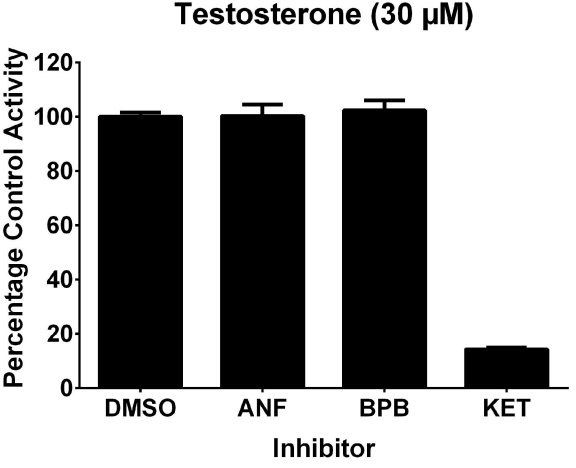
Testosterone (30 μM)
Percentage Control Activity
120
100
80
60
40
20
0
DMSO
ANF
BPB
KET
Inhibitor

Figure 4

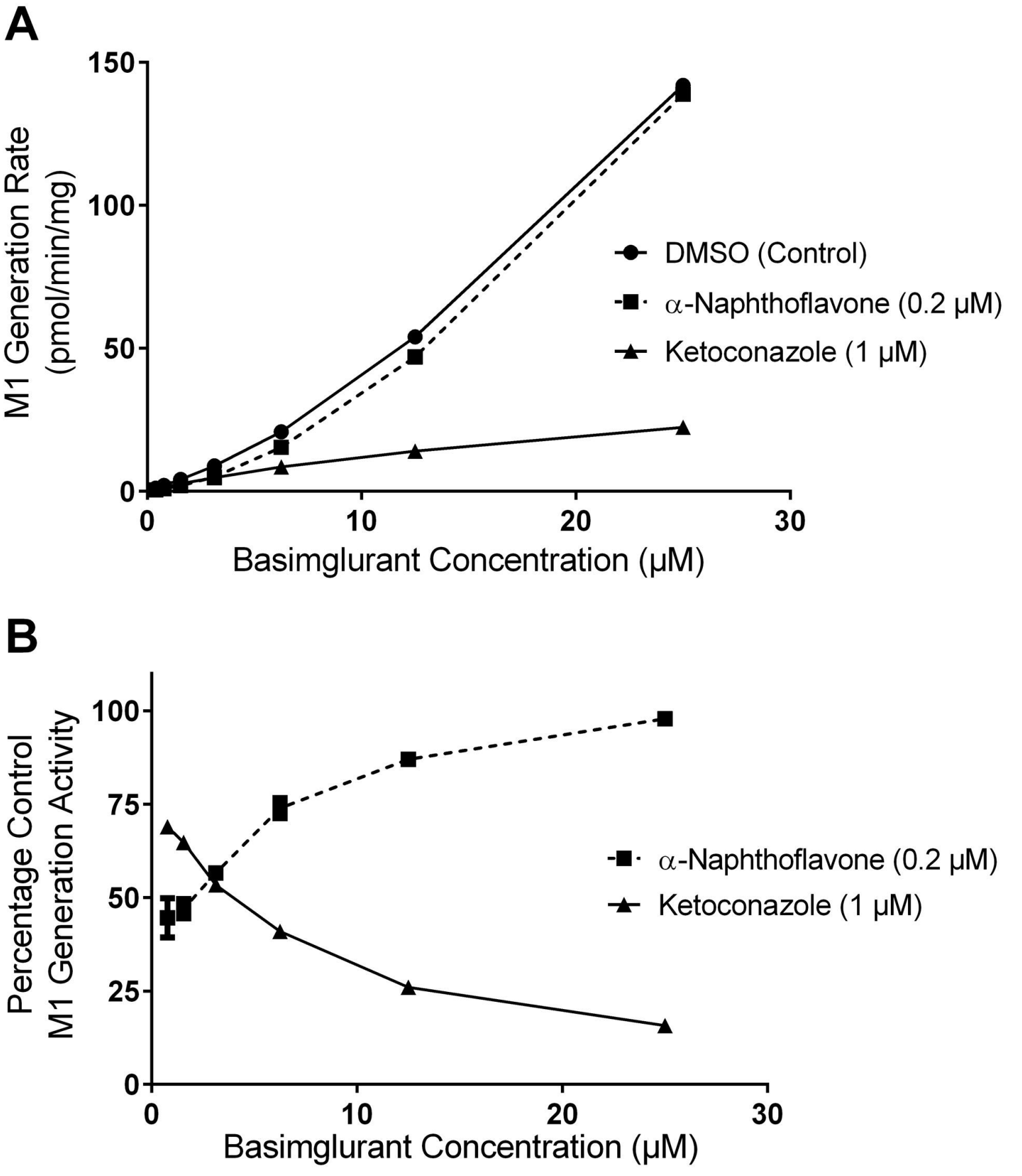
A
150
100
50
0
M1 Generation Rate
(pmol/min/mg)
DMSO (Control)
α-Naphthoflavone (0.2 μM)
Ketoconazole (1 μM)
0
10
20
30
Basimglurant Concentration (μM)
B
100
75
50
25
0
Percentage Control
M1 Generation Activity
α-Naphthoflavone (0.2 μM)
Ketoconazole (1 μM)
0
10
20
30
Basimglurant Concentration (μM)

Figure 5

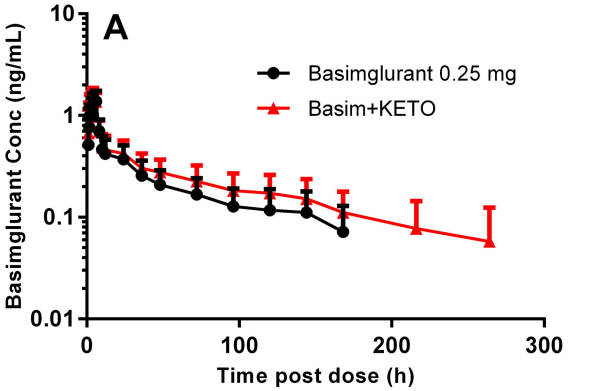
A
Basimglurant 0.25 mg
Basim+KETO
Basimglurant Conc (ng/mL)
10
1
0.1
0.01
0
100
200
300
Time post dose (h)

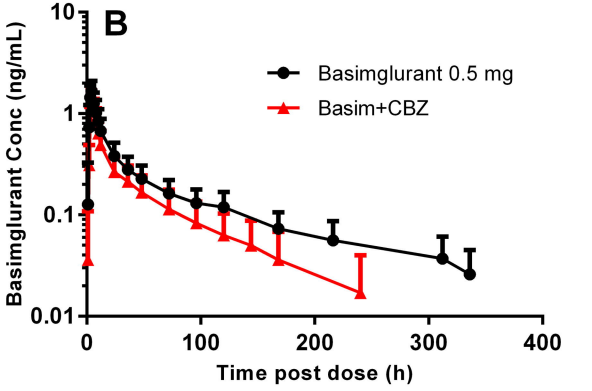
B
Basimglurant 0.5 mg
Basim+CBZ
Basimglurant Conc (ng/mL)
10
1
0.1
0.01
0
100
200
300
400
Time post dose (h)

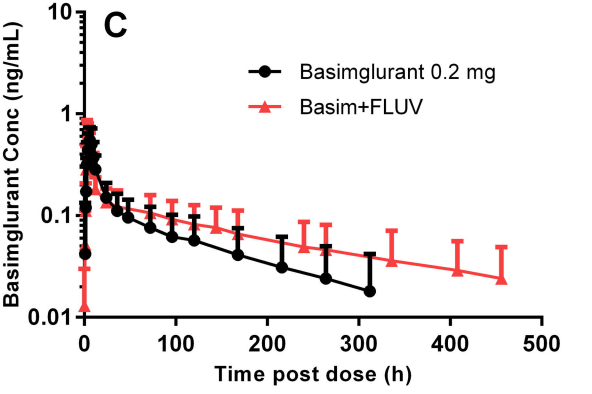
C
Basimglurant 0.2 mg
Basim+FLUV
Basimglurant Conc (ng/mL)
10
1
0.1
0.01
0
100
200
300
400
500
Time post dose (h)

Figure 6

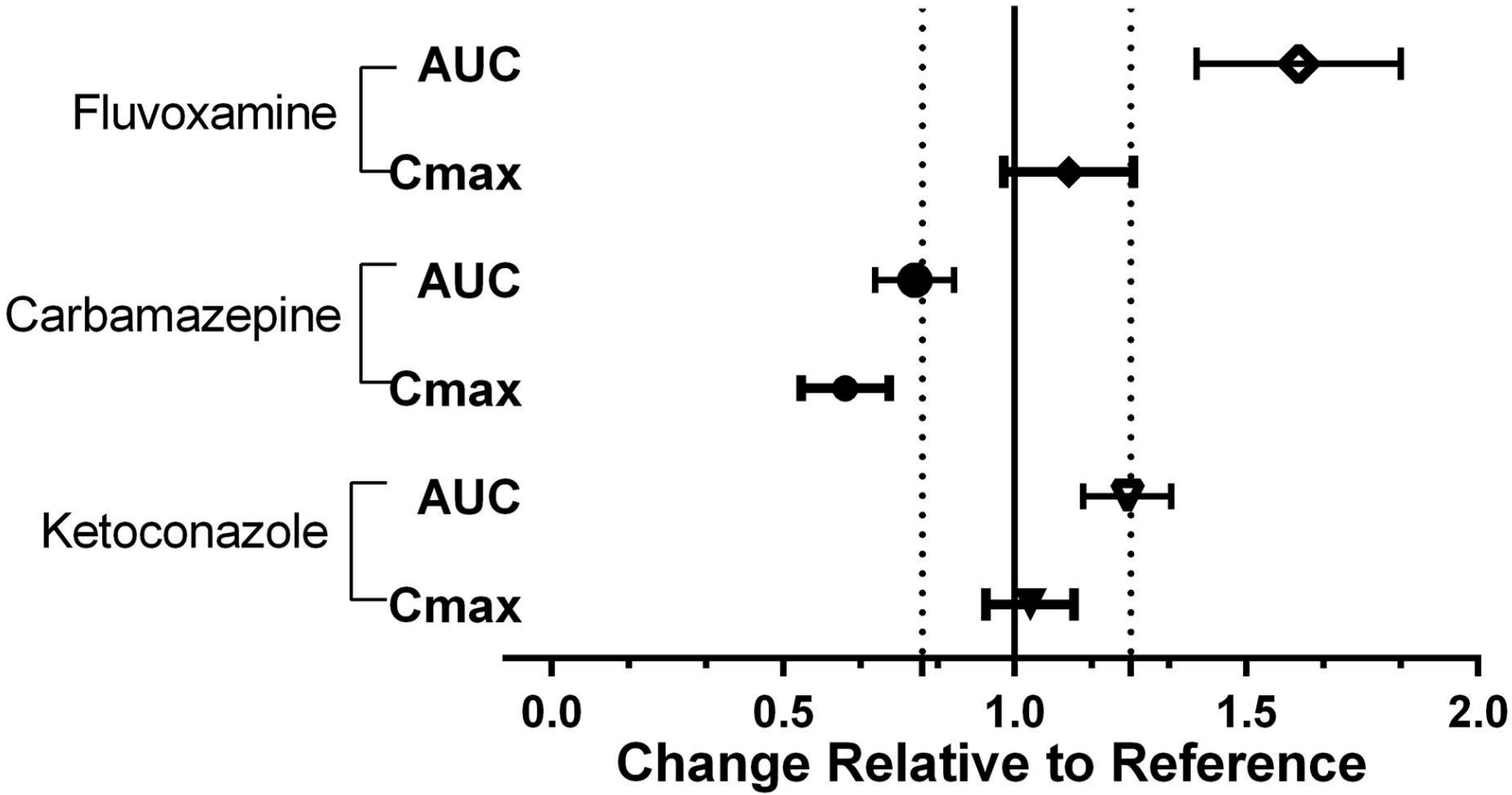
Fluvoxamine
AUC
Cmax
Carbamazepine
AUC
Cmax
Ketoconazole
AUC
Cmax
0.0
0.5
1.0
1.5
2.0
Change Relative to Reference